Simulation Development of an English Long Bow and Arrow System

Objective:

The objective of the project was to generate a bow and arrow simulation consistent with experimentally measured static and dynamic data for a traditional English Long Bow. Measurement data for the bow and arrow was recorded during 2013 in an effort to determine the dynamic efficiency of the various types of bows including; recurve, long, and compound. Draw Force versus Distance was measured through application of a spring scale and Position versus Time was measured through application of three synchronized high-speed cameras focusing on the flight of the arrow. The challenge presented by the project was to generate a model with identical characteristics of the aforementioned data sets through application of known bow making materials.

Governing Equations:

Bow and arrow systems operate by transforming the stored deformation energy of the bow and string into the kinetic energy of the arrow. During operation, the bow string is looped to the top and bottom ends of the bow, thereby applying an initial tension to the bow. The string is then draw to a set position, bending the bow further and increasing tension within the bow. Release of the bow string occurs at full draw and propels the arrow forward. The amount of deformation energy is directly related to the type of materials utilized during construction of the bow and string. Increased stiffness of select materials allows for greater draw strength and higher potential energy to be stored. Maximum transferal of the deformation energy to the arrow allows for higher kinetic energies within the arrow and therefore increased dynamic efficiency of the system.

The static and dynamic equations of drawing and then firing the bow were located from B.W. Kooi's PhD-thesis "On the Mechanics of the Bow and Arrow". Within the document, Kooi details how the static action of drawing the bow can be idealized as a modified Bernoulli-Euler equation with consideration of large deformation [4] [5]. Special attention was focused on the relative angle of the bow string to the bow during Kooi's calculations and the mass of the string was assumed negligible [5]. Also, the modified Bernoulli-Euler equations represented system dynamics. The moments, reaction forces, and energies were stated to occur over the sum of the bow limb and string [5] [6]. The idealizations made by Kooi were also stated as valid for the following model generation and used for general understanding of the problem. The formulation and derivation of the equations was not computed for the project.

Computation of the kinetic energy and dynamic efficiency were developed with respect to the bow and arrow system. The kinetic energy of the arrow equated to the mass of the arrow, $\frac{1}{2} * m_{arrow}$ multiplied by the velocity of the arrow, V_{arrow};

$$KE_{arrow} = \frac{1}{2} * m_{arrow} * V_{arrow}.$$

Lastly, the dynamic efficiency of the long bow was computed by dividing the arrow kinetic energy by the stored potential energy in the bow;

$$Dynamic\ Effeciency = \frac{Arrow\ Kinetic\ Energy}{Bow\ Stored\ Potential\ Energy}.$$

Long Bow Dimensions and Material Selection:

Measurements for the long bow were conducted to determine the maximum dimensions for the model and are shown within Table 1. Investigation of the long bow showed that the bow comprised of five unknown material layers of varying thickness laminated together. Determination of the layer thickness was extremely difficult due to the application of similar color and compression between each layer. The lamination material was also unknown. The height of the bow was also determined to have an increased thickness at the center and taper towards the end of the limbs. In addition to the tapering of the thickness, the width of the bow also decreased moving from the center to the outer edges.

Table 1: The following table details the measured dimensions for the English Long Bow. The stated dimensions were then applied to model generation in Abaqus.

Parameter	***Dimensions (meters)***
Length	1.7272 (68.0 in)
Width	0.041275 (1.625 in)
Height	0.009525 (0.375 in)

Material parameters for the bow, bowstring, and arrow were chosen based upon observation of the long bow and research of construction materials applied to modern bows. Table 2 details the utilized materials for the model. As shown, hickory wood, bamboo wood, and fiberglass were considered as the primary construction materials for the bow. Bow string material was chosen to be SK90 Dyneema, a common polyethylene fiber used in modern bow strings [6]. Lastly, the bonding material of the bow utilized during lamination of the materials was assumed to be negligible for model creation due to the understanding that the relative quantity of material would be much less than any of the materials show in Table 2.

Table 2: Material parameters for English Long Bow construction [1] [2] [3] [6] [8].

Material	***Application***	***Density (kg/m^3)***	***Young's Modulus (GPa)***	***Poisson's Ratio***
Hickory Wood	Bow Limb	1100	14.9	0.25
Bamboo Wood	Bow Limb	800	18.8	0.20
Fiberglass	Bow Limb	1500	10.1	0.10
Dyneema (PE)	Bow String	975	172.0	0.28
Aluminum	Arrow	1350	70.0	0.30

Model Component Design and Material Application:

Initial model generation of the Long Bow was provided by Professor Bower. The bow was modeled as a single rectangular wire element. Modifications to the profile of the bow were conducted to match the width and height values within Table 1. The observed tapering for both the height and width of the bow were ignored for the simulation. The bow string and arrow were modeled as wire elements with a circular profile. As with the bow limb, the profiles were altered to match measurement values. The models of the bow and string were considered symmetric and therefore only half of the model was generated to decrease overall computational time. Arrow mass was stated to be 0.031 kg for both measured and simulation computations. Profile dimensions for the three components are shown within Table 3.

Table 3: Profile assignments for components within model.

Component	*Profile*	*Height (m)*	*Width (m)*	*Radius (m)*
Bow	Rectangular	0.0127	0.041275	N/A
Arrow	Circular	N/A	N/A	0.004572
String	Circular	N/A	N/A	0.0015875

Material allocation for the bow presented significant difficulty during the simulation. Assigning multiple sections to bow resulted in computational errors and failed attempts to obtain the required simulation data. As such, the material for the bow was considered homogenous and a weighting scale was assigned to the respective materials stated in Table 2. The percentage values were assigned based upon the number of layers located within the long bow observed during dimension measuring. Table 4 details the resulting percentage assignments of the respective materials. The assumption to utilize a homogenous material is inconsistent with actual construction of a bow and corrective actions for the further studies are discussed within the conclusion.

Table 4: Percent assignments for the homogenous bow material model representation.

Material	*Percent Applied*	*Resulting Thickness (m)*	*Resulting Density (kg/m^3)*	*Resulting Young's Modulus (Pa)*	*Resulting Poisson's Ratio*
Hickory Wood	0.05	0.00206375	55	745.0 * 10^6	0.013
Bamboo Wood	0.60	0.24765	480	112.8 * 10^7	0.120
Fiberglass	0.35	0.01444625	525	385.0 * 10^8	0.035
Resulting Homogenous Material	1.00	0.041275	1060	50.525 * 10^9	0.170

Assembly, Steps, and Boundary Conditions:

The bow and arrow model was previously assembled by Professor Bower, as shown in Figure 1. Due to the symmetry condition of the problem, the assembly represents half of the total system bow. Also, the arrow was considered to be center shot from the bow thereby avoiding the buckling occurrence of the arrow, commonly referred as the Archer's Paradox.

Firing of the bow and arrow model was completed through the application of a sequence of steps. With each step, the bow and arrow system's boundary conditions were altered to simulate the following procedure; (1) stringing of the bow, thereby providing initial tension to the bow limb; (2) drawing the bow string to a predetermined distance of 0.63 m, representing full draw of the bow; (3) releasing of the bow string, representing firing of the system. The boundary conditions were altered during each step to restrict movement by the components to the X and Y direction of the system. The bow string was considered to travel perpendicular to the starting position and not bend during the draw of arrow. In addition, the arrow was restricted to only travel in the Y-direction during the draw and after release of the bow string. Figures 1 through 4 show the complete sequence of firing for the bow.

Ryan Carlson
12/16/2015

Figure 1: The above figure displays the strung bow and arrow system. The image displays the relative displacement of the model.

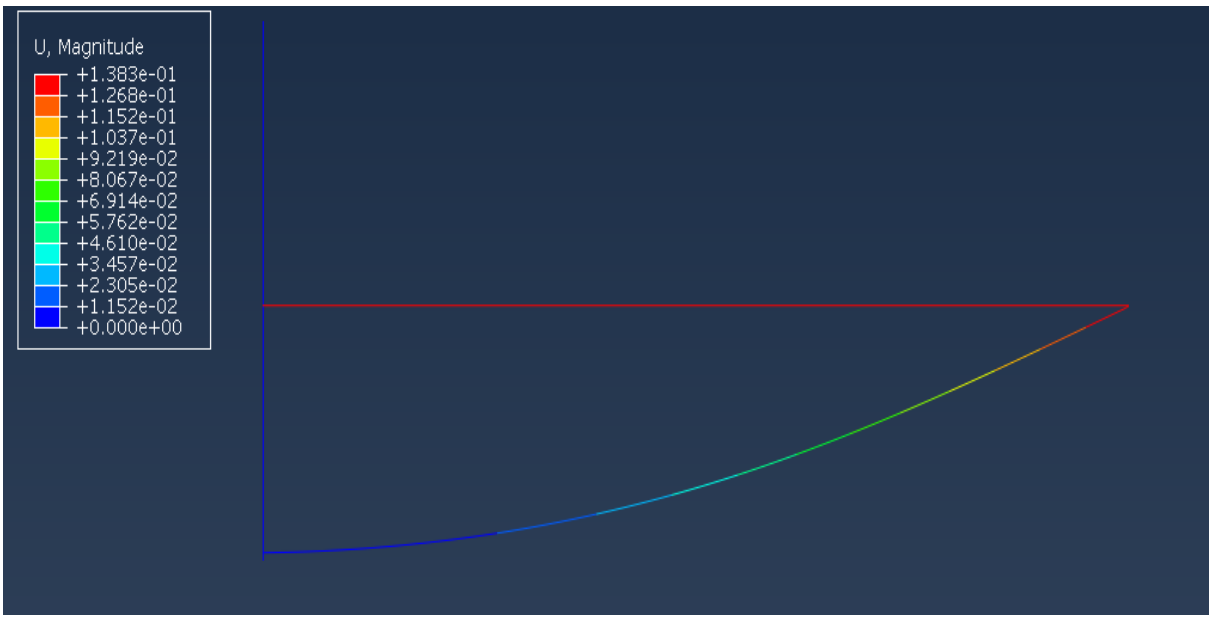

Figure 2: The preceding image details the bow and arrow system at half draw. The image displays the relative displacement of the model.

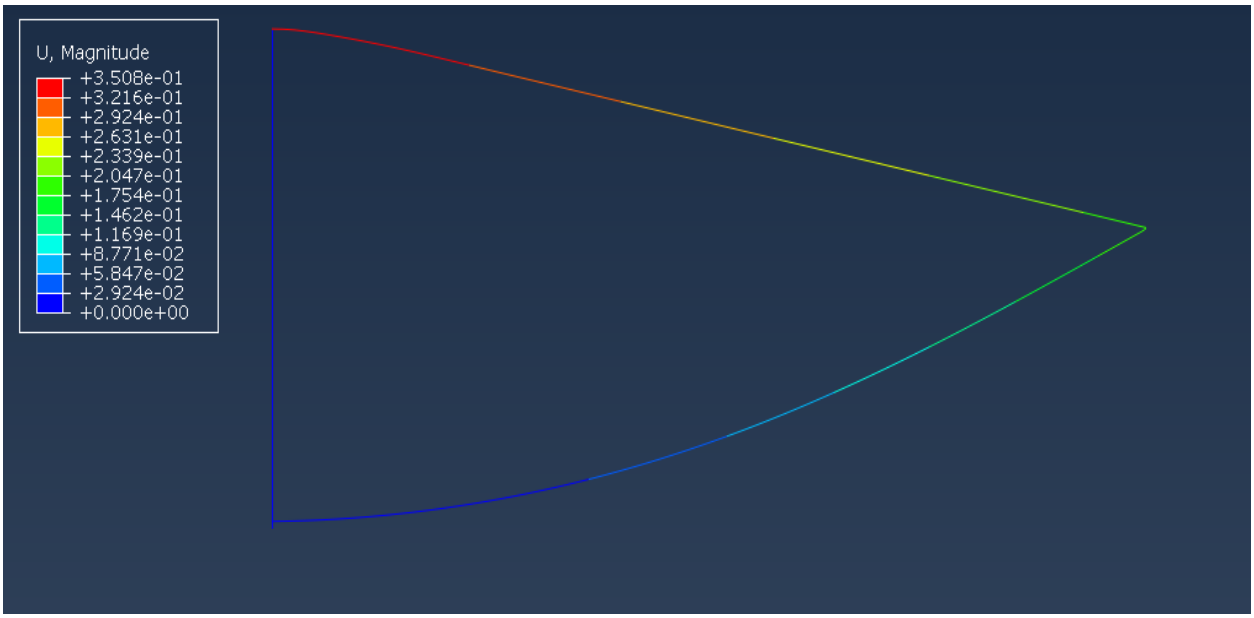

Figure 3: Bow and arrow system at a full draw length. The image displays the relative displacement of the model.

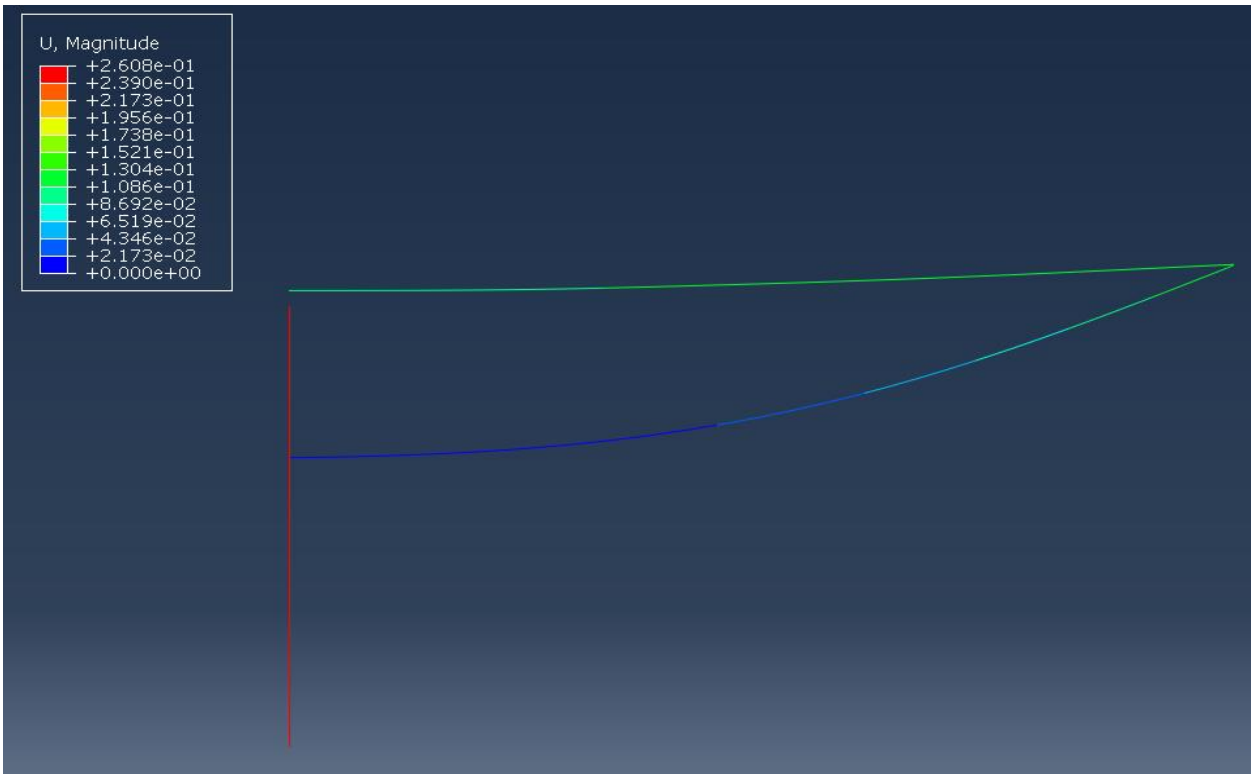

Figure 4: The above image details the release of the arrow from the bow.

Measured and Simulated Results:

Initial simulation data representing the static and dynamic characteristics of the symmetric representative model were collected for the long bow. The simulation data was then modified to correct for time biases during the analysis by subtracting all simulation time values by 2.0 seconds. The resulting adjusted data was then directly compared to the measured long bow data. As shown in Figures 5 through Figure 7, the simulation model showed similar slope behavior for the Draw Force vs. Position, Arrow Position vs. Time, and Arrow Velocity vs. Time. Averaged percent differences for the data sets were calculated to determine initial accuracy of the model and are shown within Table 5.

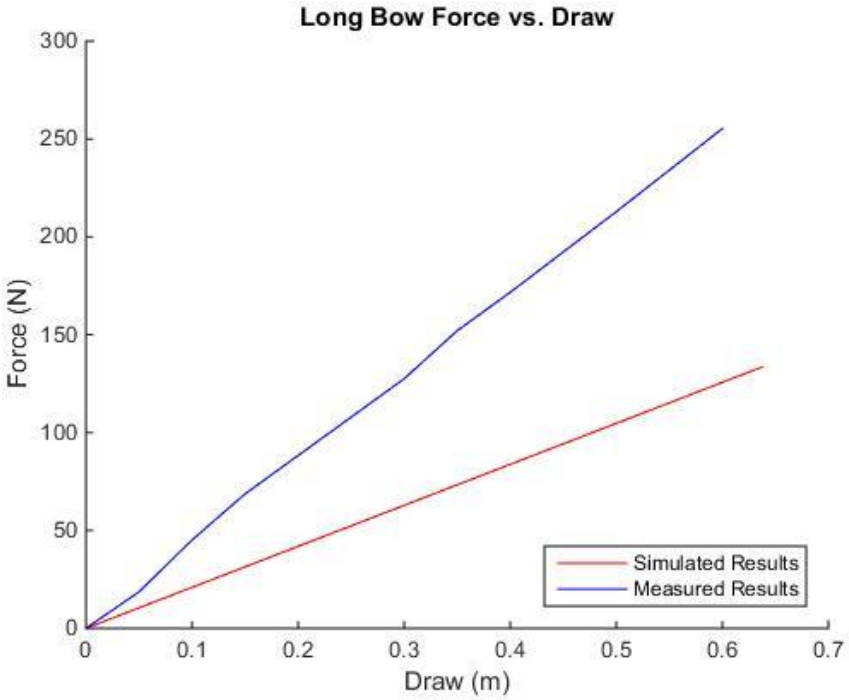

Figure 5: The above figure details the comparison between the experimental measurement data and simulation data for the static measurement of Draw Force vs. Position, prior to application of the symmetry correction factor.

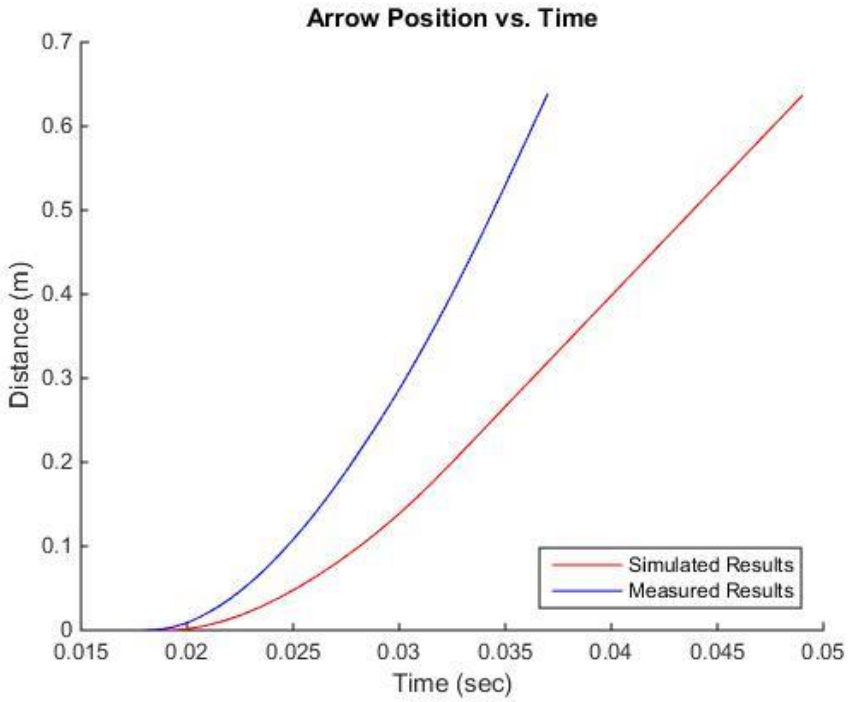

Figure 6: The preceding figure displays the comparison between the experimental measurement data and corrected simulation data for the dynamic measurement of the Arrow Position vs. Time, prior to application of the symmetry correction factor.

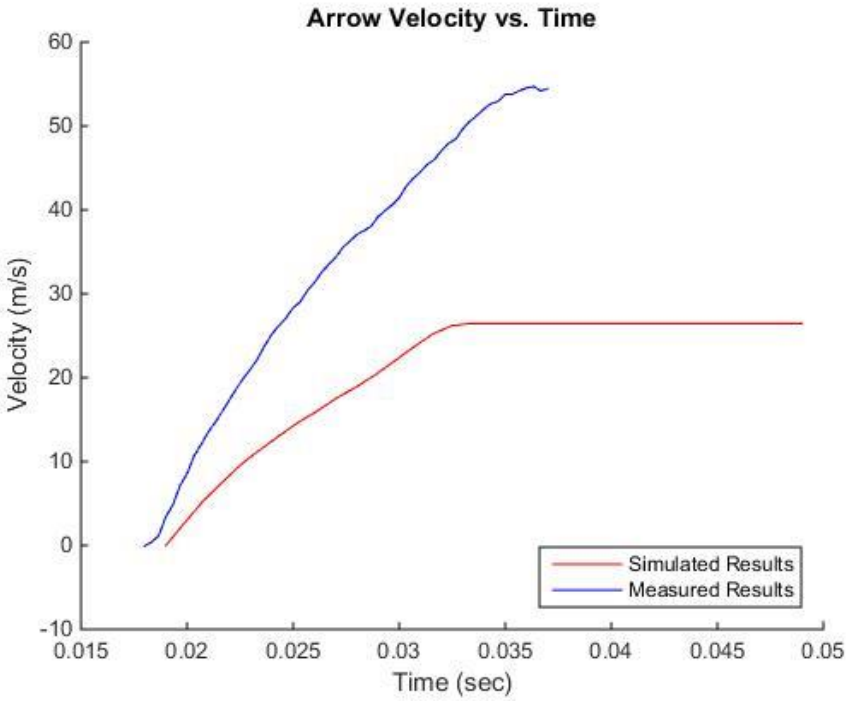

Figure 7: The above figure details the resulting Arrow Velocity vs. Time for the experimental measurement data and simulation data, prior to application of the symmetry correction factor.

Table 5: The following table contains the averaged percent difference for Figures 5-7 for both the measured and simulated data values, prior to application of symmetry correction factor.

Parameter	***Measured***	***Simulated***	***Percent Diff.***
Draw Force vs. Position	128.80 N	66.85 N	48.10 %
Arrow Position vs. Time	0.233 m	0.120 m	48.51 %
Arrow Velocity vs. Time	32.99 m/s	17.86 m/s	45.88 %

A correction value of 2.0 was applied to account for the symmetry of the bow and arrow system. The corrected simulation data was then plotted with the measured results, as shown in Figures 8 through 10. The simulation data was also corrected to have the same time range as the measured data to increase calculation accuracy. The assumption to alter the time range was considered valid under the reasoning that the simulation was linear beyond the specified time of 0.038 seconds.

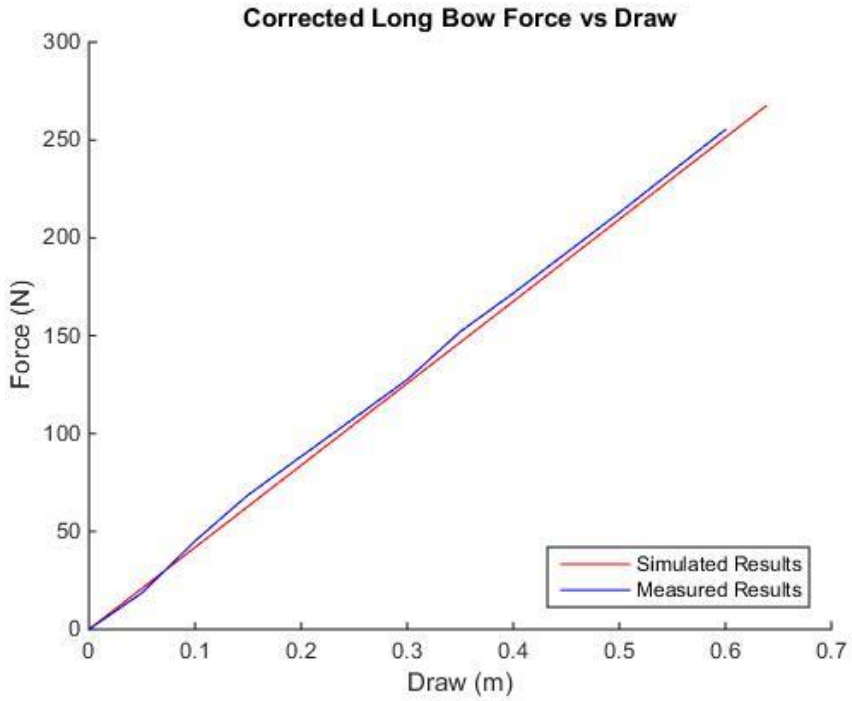

Figure 8: The preceding image details the comparison between the experimental measurement data and simulation data for the static measurement of Draw Force vs. Position, with the application of a correction factor of 2.0 to account for the symmetry of the bow and arrow system.

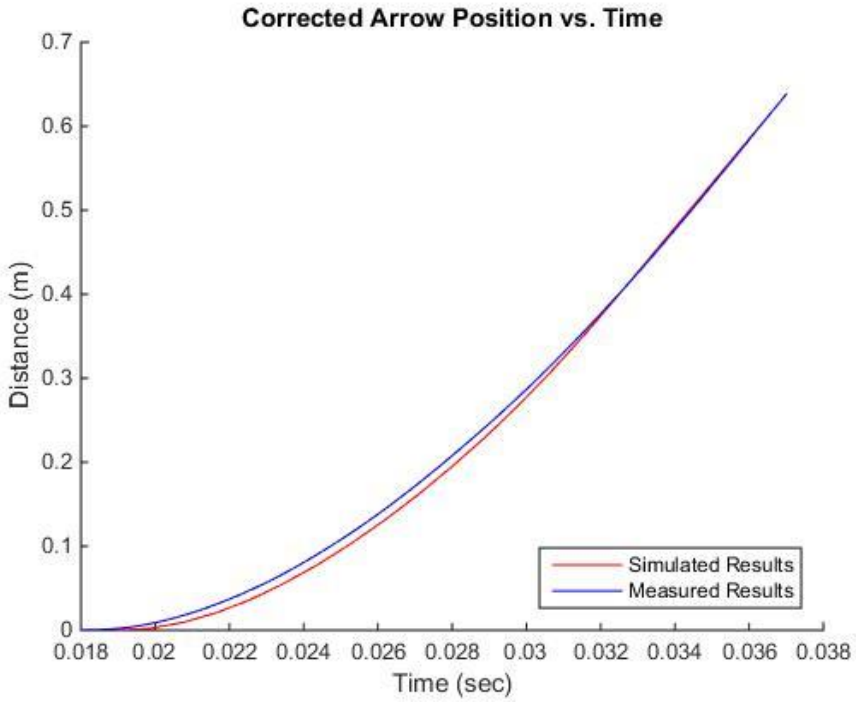

Figure 9: The preceding figure displays the comparison between the experimental measurement data and simulation data for the dynamic measurement of the Arrow Position vs. Time, with the application of a correction factor of 2.0 to account for the symmetry of the bow and arrow system.

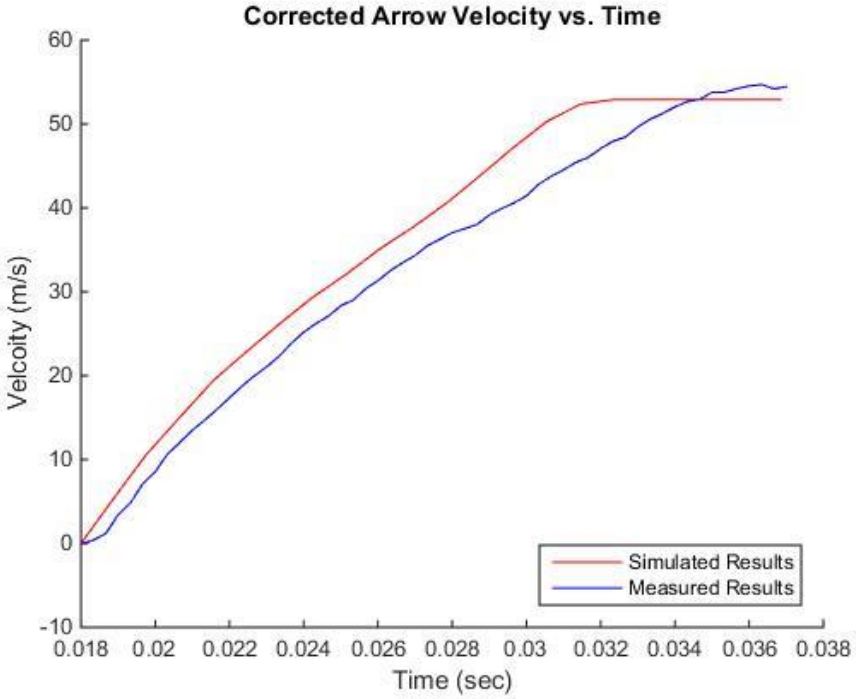

Figure 10: The above figure details the resulting Arrow Velocity vs. Time for the experimental measurement data and simulation data, with the application of a correction factor of 2.0 to account for the symmetry of the bow and arrow system.

Table 6: Averaged percent differences were computed for Corrected Draw Force vs. Position, Corrected Arrow Position vs. Time, and Corrected Arrow Velocity vs. Time.

Parameter	***Measured***	***Simulated***	***Percent Diff.***
Corrected Draw Force vs. Position	128.80 N	133.70 N	3.81 %
Corrected Arrow Position vs. Time	0.233 m	0.240 m	2.98 %
Corrected Arrow Velocity vs. Time	32.99 m/s	35.71 m/s	8.23 %

Dynamic efficiency, represented by the ratio of kinetic energy of the arrow to the stored energy value in the bow, were calculated for both the simulated and measured long bow. Velocities required for the calculation were approximated from the linear portion of the Corrected Arrow vs. Time graphs. Potential energy of the bow was determined through application of Matlab's trapz function for the Arrow Position vs. Time graph. Table 7 details the bow's potential energy, velocity of arrow, and kinetic energy of arrow for both the measured and simulated data. The aforementioned data along with Equations 1-3 were applied to determine the dynamic efficiency of the bow. The dynamic efficiency of the measured and simulated long bow were 64.73 % and 67.64%, respectively. The simulation showed a 4.50 % difference as compared to the measured data.

Table 7: The following table details the determined values of the bow's potential energy, velocity of arrow, kinetic energy of arrow, and resulting dynamic efficiency.

Parameter	***Measured***	***Simulated***
Stored Potential Energy (Joules)	77.34	85.35
Velocity of Arrow (m/s)	50.60	54.34
Kinetic Energy of Arrow (Joules)	50.06	57.73
Dynamic Efficiency (%)	64.72	67.64

Conclusion:

The simulation of the English Long Bow through application of the homogenous material characteristics and with a correction factor to account for symmetry created a realistic representation to the measured data. Percent difference for the dynamic efficiency for the bow and arrow simulation equated to 4.50 % as compared to the measured system. In addition, the percent differences of the Corrected Draw Force vs. Position, Corrected Arrow Position vs. Time, and Corrected Arrow Velocity vs. Time were all below 9.00%. Further refinement of the material parameters within the simulated bow and arrow system would decrease the respective percent differences.

For further study, the bow should not be considered as a homogenous material with the respective assigned weights. The bow should be delimitated and each individual layer should be investigated to determine exact width and material. The lamination material to hold the bow layers together should also be determined. Lastly, the manufacture of the bow should be contacted to obtain exact material property values. The next iteration of the model should also have tapering profiles as the bow progresses towards the outer limbs, allowing for an adjustment to the potential energy levels of the bow. In addition to the aforementioned aspects, modeling the bow to investigate the Archer's Paradox would generate a more realistic simulation as compared to the measured results.

Works Cited

1. "ASM Material Data Sheet." *ASM Material Data Sheet*. N.p., n.d. Web. 15 Dec. 2015.
2. "Bamboo." *The Wood Database*. N.p., n.d. Web. 15 Dec. 2015.
3. "Dyneema Material." *Dyneema*. N.p., n.d. Web. 15 Dec. 2015.
4. "Euler–Bernoulli Beam Theory." *Wikipedia*. Wikimedia Foundation, n.d. Web. 15 Dec. 2015.
5. Kooi, B.W. "On The Mechanics of the Bow and Arrow." *On the Mechanics of the Bow and Arrow PhD-thesis, M* (1983): 1-176. Web. 14 Dec. 2015.
6. "Learning Center - Fundamentals of Fiberglass." *Fiber Glass*. N.p., n.d. Web. 15 Dec. 2015.
7. Marlow, W.C. "Bow and Arrow Dynamics." *The Perkin-Elmer Corporation* (1980): n. page. Web. 15 Dec. 2015.
8. "Shagbark Hickory." *The Wood Database*. N.p., n.d. Web. 15 Dec. 2015.